Mechano-capacitive properties of polarized membranes and the application to conductance measurements of lipid membrane patches

Zecchi, Karis Amata; Mosgaard, Lars Dalskov; Heimburg, Thomas Rainer

Published in:
Journal of Physics: Conference Series

DOI:
10.1088/1742-6596/780/1/012001

Publication date:
2017

Document version
Publisher's PDF, also known as Version of record

Mechano-capacitive properties of polarized membranes and the application to conductance measurements of lipid membrane patches

IOP Conf. Series: Journal of Physics: Conf. Series **780** (2017) 012001 doi:10.1088/1742-6596/780/1/012001

Mechano-capacitive properties of polarized membranes and the application to conductance measurements of lipid membrane patches

Karis A Zecchi, Lars D Mosgaard and Thomas Heimburg*

Niels Bohr Institute, University of Copenhagen, Blegdamsvej 17, 2100 Copenhagen Ø, Denmark

E-mail: theimbu@nbi.ku.dk

Abstract. Biological membranes are capacitors that can be charged by applying an electric field across the membrane. The charges on the capacitor exert a force on the membrane that leads to electrostriction, i.e., a thinning of the membrane. This effect is especially strong close to chain melting transitions. A consequence is voltage induced pore formation in the lipid membrane. Since the force is quadratic in voltage, negative and positive voltages have an identical influence on the physics of symmetric membranes. This is not the case for a membrane with an asymmetry leading to a permanent electric polarization. Positive and negative voltages of identical magnitude lead to different physical properties. Such an asymmetry can originate from a lipid composition that is different on the two monolayers of the membrane, or from membrane curvature. The latter effect is called flexoelectricity. It was investigated in detail by A.G. Petrov in the recent decades. As a consequence of permanent polarization, the membrane capacitor is discharged at a voltage different from zero. This leads to interesting electrical phenomena such as outward or inward rectification of membrane permeability. The changes in current-voltage relationships are consistent with the known magnitude of the flexoelectric effect.

1. Introduction

The major components of biological membranes are lipids and proteins. Lipids are amphiphilic molecules with hydrophobic chains and polar head groups. When exposed to water, they spontaneously form membranes, which are thin layers with a thickness of approximately 5 nm. Biological membranes resemble artificial membranes but have proteins embedded into them. They are surrounded by electrolytic buffers containing ions that can associate with the surface. Therefore, membranes are excellent capacitors. Biological membranes usually are asymmetric. For instance, they frequently possess a larger concentration of charged lipids on the inner layer of a biological membrane. Asymmetric proteins can contribute to such an electrical asymmetry, and so can asymmetric ion distributions due to the interaction of ions with lipids. Such effects lead to a net polarization of the membrane. A further effect leading to polarization is membrane curvature. This effect is called flexoelectricity and was described in much detail by A. G. Petrov (e.g.,[1]).

Many functions of biological membranes are associated with electrical phenomena. For instance, the nerve pulse consists of a propagating pulse in membrane voltage and polarization [2]. Traditionally, the electrical phenomena are attributed to the function of certain proteins

called ion channels [3]. However, it has been shown that the lipid layer alone can support electrical pulses [4, 5, 6, 7]. Further, in electrophysiological models it is usually assumed that the membrane capacitance is constant, and that the membrane is an electrical insulator. Both assumptions are incorrect. Biological membranes possess melting transitions close to physiological temperatures, where the order of both the lipid chains and the lateral molecular arrangement decreases. In these transitions, both membrane area and thickness changes, giving rise to changes in capacitance by at least 50% [8]. Further, membranes are in fact quite permeable in this temperature regime, and one finds electrical conductance traces that resemble those of ion channel proteins (e.g., [9, 10, 11]). As a consequence, the membrane can display interesting nonlinear conductance phenomena that are similar but not related to the properties ascribed to proteins [12].

In this report we show the temperature-dependent changes in membrane capacitance. Further, we theoretically discuss the emergence of polarization effects in the lipid membrane, that lead to flexoelectricity and a net membrane polarization. These phenomena are used to describe non-linear electrical conductance phenomena that are not symmetric upon reversal of voltage.

2. Materials and Methods

2.1. Chemicals and membranes

1,2-dimyristoyl-*sn*-glycero-3-phosphocholine (DMPC), 1,2-dilauroyl-*sn*-glycero-3-phospho-choline (DLPC),1-palmitoyl-2-oleoyl-*sn*-glycero-3-phosphocholine (POPC), 1-palmitoyl-2-oleoyl-*sn*-glycero-3-phosphoethanolamine (POPE) and cholesterol were purchased from Avanti Polar Lipids (Alabaster/AL, US) and used without further purification. In the experiments shown here two lipid mixtures were used: POPE:POPC=8:2 (mol:mol) for the capacitance measurements and a 10:1=DMPC:DLPC (mol:mol) mixture in the absence and presence of 15% cholesterol (mol/mol of total lipid) for the current-voltage curve measurement.

The 150 mM KCl electrolyte solution used for the BLM experiments was buffered with 2 mM HEPES and 1 mM EDTA (both from Sigma Aldrich, Germany), pH 7.4. For the patch clamp experiments, the electrolyte was made of 150mM KCl, 150 mM NaCl and 50 mM TRIS (Sigma Aldrich, Germany) and the pH was 7.6. All water used in the experiments was purified with a Direct-Q® Water Purification System (Merck Millipore, Germany) and had a resistivity >18.1 MΩ·cm. Electrolyte solutions were filtered through a sterile 0.2 μm filter (Minisart® Sartorius Stedim Biotech, Germany) to get rid of dust particles or impurities (this is particularly important in experiments with glass pipettes of small aperture).

2.2. Black lipid membrane (BLM) setup

The DMPC:DLPC:cholesterol = 77.3:7.7:15 (mol:mol:mol) mixture used for the current-voltage (I-V) measurements and the POPE:POPC = 8:2 (mol:mol) mixture used for the capacitance measurements on the Black Lipid Membrane (BLM) setup were both dissolved in decane to a final concentration of 10 mg/mL. Planar lipid bilayers were formed on a circular aperture in a 25 μm thick Teflon film using a slightly modified version of the painting method introduced by Mueller et al [13]. The original method consists in painting a small volume of the lipid solution on the hole of a Teflon film separating two chambers filled with an electrolyte solution. The membrane is then allowed to thin out for a few minutes until a bilayer is formed which is in equilibrium with a surrounding annulus made of the bulk lipid solution (the so called Plateau-Gibbs border), as shown in figure 1 (left). In this particular example, the hole had a diameter of 120 μm, and the membrane patch a diameter of ⌀=86 μm. More details on the different methods for bilayer formation can be found in [14]. Here we used commercially available horizontal bilayer slides (Ionovation GmbH, Germany) made of two microchambers (filled with approx 150 μL of the same electrolyte solution) separated by an horizontal Teflon film. The upper and lower

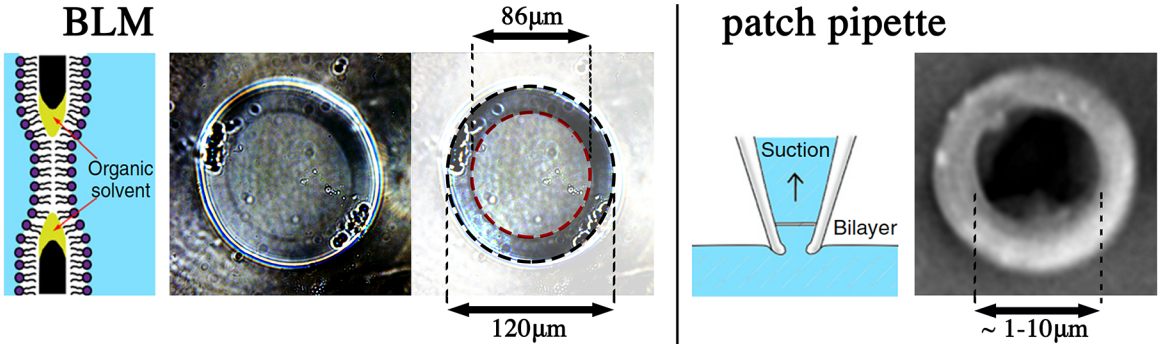

Figure 1. Left: Schematic drawing [14] and image of black lipid membrane. The outer diameter of the hole (∼120 µm) and the diameter of the membrane (∼86 µm) are highlighted by dashed lines. Right: Schematic drawing of a membrane in a patch pipette, and microscopic image of a patch pipette tip with diameter of ∼1- 10 µm diameter.

chambers are connected only through the 120µm aperture in the film and each has an access port for the electrical connections and for buffer perfusion. Once a small droplet ($\simeq$ 0.2 µL) of lipid solution is placed in the upper chamber close to aperture, a bilayer is formed automatically by a microfluidic perfusion system (Ionovation Explorer, Ionovation GmbH, Germany). The membrane formation was monitored with capacitance measurements and was automatically repeated until the membrane capacitance was stable above a minimum threshold value of 40 pF. The bilayer slide was placed on the work stage of a in inverted microscope (IX70, Olympus, Japan) which allowed for optical monitoring of the bilayer formation.

2.3. Calorimetry

Heat capacity profiles were recorded using a VP-DSC (MicroCal, Northampton/MA, USA - now part of Malvern Instruments Ltd. ,Worcestershire , UK) with a scan rate of 5°/h.

2.4. Patch Clamp Setup

The mixture of 10:1 = DMPC:DLPC (mol:mol) was resuspended in a highly volatile solvent made of 4:1=hexane:ethanol (vol:vol) to a final concentration of 2mM. Synthetic lipid membranes were formed on the tip of a patch-clamp glass pipette using the droplet method introduced by Hanke [15, 14], in which a droplet of the lipid solution is placed on the outer surface of a vertically standing glass pipette filled with the electrolyte solution. The tip of the pipette is in contact with the surface of a beaker containing the same electrolyte solution as the pipette, and as the droplet flows down the glass surface, it seals the pipette tip with a spontaneously formed bilayer. The solvent is the allowed to diffuse out of the bilayer for about 30s before starting the experiments. The whole experimental procedure for the patch clamp setup followed the one used and explained in [16, 17]. A microscopic image of the tip of a patch pipette is shown in figure 1 (right). Typical membrane patches have a diameter between 1 and 10 µm. Thus, they are much small than the BLMs.

3. Theory

3.1. Capacitance

The capacitance of a membrane is given by

$$C_m = \varepsilon_0 \varepsilon \frac{A}{d} \,, \tag{1}$$

where A is the membrane area, d its thickness, $\varepsilon_0 = 8.8541878 \cdot 10^{-12}$ F/m is the vacuum permittivity, and ε is the dielectric constant (assumed to be 3 for the hydrophobic core of the membranes). In the melting transition of a lipid membrane made of DPPC, the area changes by 24% and the thickness by -16%. Therefore, the calculated capacitance increase is 49% upon scanning through the melting transition [8].

3.2. Capacitance and polarization

Recently, we have investigated polarization effects in membranes [12]. If one considers the membrane as a capacitor, the membrane charge is given by

$$q = A(\varepsilon_0 \varepsilon E + P_0) = \varepsilon_0 \varepsilon \frac{A}{d}(\Psi + \Psi_0) = C_m(\Psi + \Psi_0) \,, \tag{2}$$

where P_0 is the permanent polarization of the membrane. The electrostatic potential difference across the membrane is $\Psi = E \cdot d$ and the offset potential related to the polarization is $\Psi_0 = (P_0/\varepsilon_0\varepsilon) \cdot d$. The latter quantity describes the membrane polarization that is present in the absence of an external field. The electrostatic free energy density of the membrane is given by [12]

$$g^{el} = -\frac{C_m}{2\,A}\left((\Psi + \Psi_0)^2 - \Psi_0^2\right) \,, \tag{3}$$

which is zero at zero voltage.

3.3. Flexoelectricity

From equation 2 it follows for the curvature dependence of the charge on the membrane capacitor (at constant temperature, membrane area and constant voltage)

$$dq = \left[(\Psi + \Psi_0)\underbrace{\left(\frac{\partial C_m}{\partial c}\right)_\Psi}_{\equiv\alpha} + C_m \underbrace{\left(\frac{\partial \Psi_0}{\partial c}\right)_\Psi}_{\equiv\beta}\right] dc \equiv \left[(\Psi + \Psi_0)\alpha + C_m\beta\right] dc \,, \tag{4}$$

where α and β are constant coefficients. The curvature is given by $c = 1/R$, where R is the radius of curvature. If the capacitance is constant ($\alpha = 0$), the integral of the above yields

$$q(c) = C_m\left(\Psi + \Psi_0(0)\right) + C_m\beta \cdot c \,, \tag{5}$$

where $C_m\left(\Psi + \Psi_0(0)\right)$ is the membrane charge at $c = 0$ (equation 2). In the absence of an applied voltage ($\Psi = 0$), and when the membrane is not polarized in the absence of curvature ($\Psi_0(0) = 0$) we obtain

$$q(c) = C_m\beta \cdot c \qquad \text{or} \qquad \Psi_0(c) = \beta \cdot c \,, \tag{6}$$

making use of $q/C_m = \Psi_0$ for $\Psi = 0$ (equation 2). Thus, the offset potential Ψ_0 is proportional to the curvature. This relation is a special case of the flexoelectric effect described in equation (4). A. G. Petrov discussed this effect in many papers in the 1980s and 1990s [1]. In his nomenclature,

$$\Psi_0(c) = \frac{f}{\varepsilon_0\varepsilon} \cdot c \,. \tag{7}$$

If the membrane is curved along two axes, this has to be replaced by $\Psi_0(c) = (f/\varepsilon_0\varepsilon) \cdot (c_1 + c_2)$. Here, the flexoelectric coefficient $f \equiv \beta \cdot \varepsilon_0\varepsilon$ is introduced. Petrov and collaborators found experimentally that $f = 1 - 4 \cdot 10^{-18}$ [C] for different membranes and mixtures [18]. Let us assume that $f = 1 \cdot 10^{-18}$ C, which leads to $\beta = 3.8 \cdot 10^{-8}$ [V· m] for $\varepsilon = 3$. For a radius of

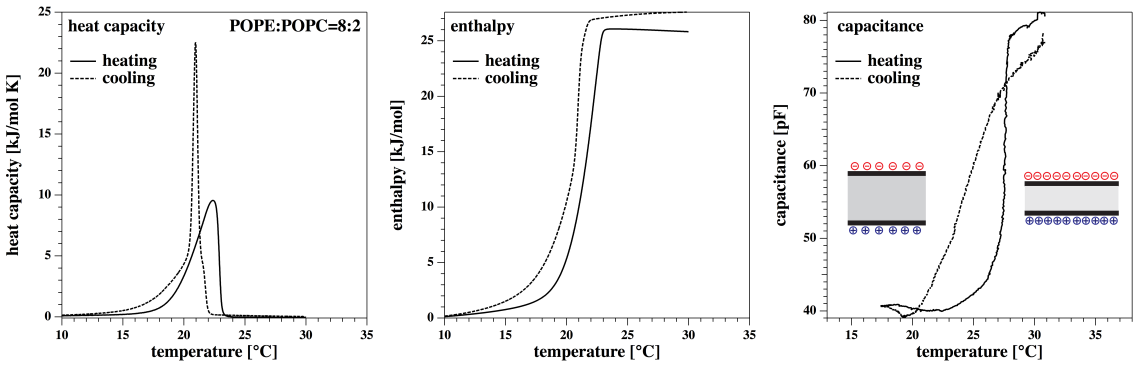

Figure 2. Left: Melting profile of a POPE : POPC = 8:2 membrane. Shown are both heating and cooling scans. Scan rate was 5°/hour. Center: The integral of the heat capacities yields the enthalpy changes. Right: In BLM experiments, one finds significant changes of the membrane capacitance of 89%.

curvature of 100 μm one finds $\Psi_0 = 380$ μV, and for a radius of curvature of 1 μm one obtains $\Psi_0 = 38$ mV. The flexoelectric effect implies that membrane curvature induces a polarization of the membrane. As mentioned, the flexoelectric coefficients were found to be very dependent on the lipid, and it is likely that it is also affected by the phase behavior of lipid mixtures. Generally, the flexoelectric effect seems to be larger in charged membranes.

3.4. Pore formation and conductance

The above concepts can be applied to understand the influence of voltage and membrane polarization on membrane permeability. The permeability of a membrane is related to the formation of small pores in the lipid membrane. The likelihood to form a pore is proportional to the square of the applied electric potential [19, 20, 17]. This assumption is based on the hypothesis that an increase in voltage thins the membrane due to an effect called electrostriction [8] and eventually leads to an electric breakdown linked to pore formation. It has been found that current-voltage (I-V) relations for a chemically symmetric phosphatidylcholine membrane patch can be either a non-linear symmetric [21], or non-linear asymmetric functions of voltage [16, 17, 12].

Blicher et al. [17] proposed that an offset potential, Ψ_0, can explain asymmetric I-V profiles. The free energy difference between an open and a closed pore, ΔG_p, can be expressed by

$$\Delta G_p = \Delta G_{p,0} + \delta \left((\Psi + \Psi_0)^2 - \Psi_0^2 \right) \ , \tag{8}$$

where $\Delta G_{p,0}$ and δ are coefficients describing the difference in free energy between open and a closed pore in the absence and the presence of externally applied voltage. The equilibrium constant between open and closed pores is given by $K_p = \exp(-\Delta G_p / kT)$, and the likelihood of finding an open pore is given by $P_{open} = K_p/(1 + K_p)$. The I-V relation can be expressed as

$$I = \gamma_p P_{open} \Psi \ , \tag{9}$$

where γ_p is the conductance of the membrane when all pores are open. A value for Ψ_0 can be determined by fitting the above set of equations to the experimentally determined I-V profile. The equations have 4 parameters, Ψ_0, $\Delta G_{p,0}$, δ, and γ_p. Only Ψ_0 has an influence on the asymmetry. Therefore, the offset potential is well-defined.

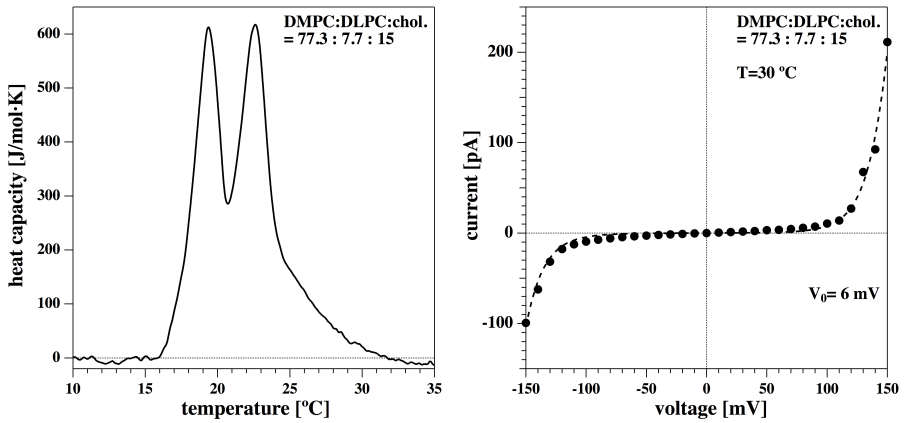

Figure 3. Electrical experiments in BLMs. Left: Melting profile of membranes made from a mixture of DMPC, DLPC and cholesterol (molar ratios 77.3:7.7:15). Right: Current-voltage relationship. It is only slightly asymmetric. The dashed line is a fit using equation 9. The offset voltage determined this way is 6mV.

4. Experimental results

4.1. Capacitance measurements

We first measured the capacitance as a function of temperature in order to demonstrate that it changes in the transition regime, and therefore is not generally constant. For a membrane made of POPE:POPE = 8:2, this effect is shown in figure 2. The left hand panel shows the heat capacity profiles obtained by heating and by cooling. The integral of the heat capacity yields the enthalpy changes, H (figure 2, center). The capacitance, measured in the BLM setup, changes by about 89 ± 6 % upon melting, roughly proportional to the enthalpy changes. It should be noted that the BLM contains decane, which is not present in the calorimetric measurement. This leads to slightly different shapes and values for the transition temperature.

In the following, we use conditions where the membranes are at the upper end of the transition.

4.2. Current-voltage (I-V) relations

In the folling we measure the current through a membrane as a function of voltage at constant temperature. Figure 3 shows a BLM experiment performed on a DMPC:DLPC:cholesterol = 77.3:7.7:10 mixture. In the BLM experiment, the aperture of the hole in the teflon film is usually large - of the order of 100 μm (cf. figure 1, left). The left hand panel of figure 3 shows a heat capacity profile. It displays two heat capacity maxima at 19.4°C and 22.6°C. The profile extends up to 30°C. The right hand panel shows an I-V profile recorded at 30°C, i.e., at the upper end of the transition. We find that is symmetric, meaning that the application of negative and positive voltages yield very similar results. The dashed line indicates a fit to eqs. 8-9. We find a small offset potential, $\Psi_0 \approx 6$ mV. We have recorded many of such profiles. It is a general observation that the I-V profiles turn out being symmetric in BLM experiments (see also [21] for a DOPC:DPPC = 2:1 mixture).

Figure 4 shows a patch pipette experiment performed on a DMPC:DLPC = 90:10 mixture. In pipette experiments, the opening of the pipette tip is usually quite small - of the order of 1 to 10 μm (cf. figure 1, right). The left hand panel of figure 4 shows a heat capacity profile with a maximum at 22.2°C. The right hand panel shows an I-V profile recorded at 24°V, which is at the upper end of the transition range. In the recording technique used by us, the pipette

touches the surface of the aqueous buffer. However, one can lower the tip of the pipette and create pressure differences between the two sides of the membrane. In the experiment, we changed the depth of the pipette in the water from 0 mm to 8 mm, corresponding to a pressure change across the membrane of 82 Pa. The I-V profile is quite symmetric in the absence of a pressure difference, while it becomes quite asymmetric upon application of a pressure difference, i.e., application of negative and positive voltages yield very different results. The latter profiles are called 'outward-rectified' meaning that the permeability increases faster with positive as compared to negative voltages. We find an offset potential of $\Psi_0 \approx 0$ mV for the experiment in the absence of a pressure difference, while we find $\Psi_0 \approx 160$ mV at 8mm depth. We often see that changes are transient. This could mean that after a sudden change in pressure material may flow and the tension on the membrane does not stay constant. When repeating this kind of measurement with patch pipettes we nearly always find asymmetric non-linear I-V profiles. It is interesting to note that the I-V profiles shown here for patch pipettes are very similar to those recorded for some membrane proteins [16, 11]. The profiles attributed to proteins as the TRP receptor proteins can equally well be fitted by the simple model leading to eqs. 8-9. Such rectified profiles have been thought to be typical for membrane proteins. However, as we show here, the rectification of I-V profiles easily originates from a polarization of the lipid membrane.

5. Discussion and conclusions

It is obvious that the current-voltage relations of BLMs and of patches on pipettes look different. While the BLM experiments regularly lead to symmetric profiles that become non-linear at higher voltage, they are usually asymmetric on patch pipettes. One can nicely fit the asymmetric profiles with an offset potential, Ψ_0. It is tempting to speculate about the origin of this polarization. One possibility to explain it is related to flexoelectricity. The different diameters of the BLM aperture and the diameter of the patch pipette tip allow for different possible membrane curvatures. In figure 5 we show the scenarios for BLM and patch pipettes. On the left side we show the possible curvatures of a membrane on the opening of a teflon hole. Obviously, a membrane that spans across the hole in a flat manner has a curvature of $c = 0$ [1/m]

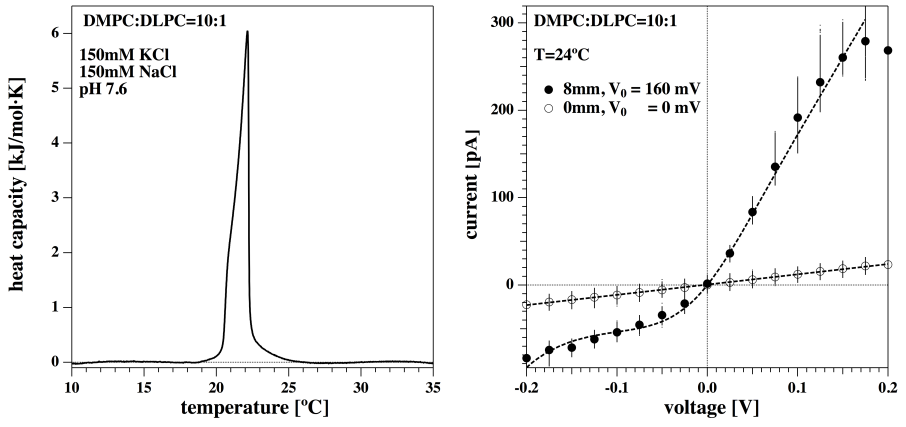

Figure 4. Electrical experiments in patches on a pipette tip. Left: Melting profile of membranes made from a mixture of DMPC and DLPC (molar ratios 90 : 10). The mixture displays one heat capacity maximum at 22.2°C. Right: Current-voltage relationship at two different pressures (difference in water depth is 8mm). If the membrane is at the surface of the aqueous interface, the I-V curve is symmetric and linear. At 8mm depth, it is asymmetric, and displays an offset potential of 160 mV. The dashed lines are fits using equation 9.

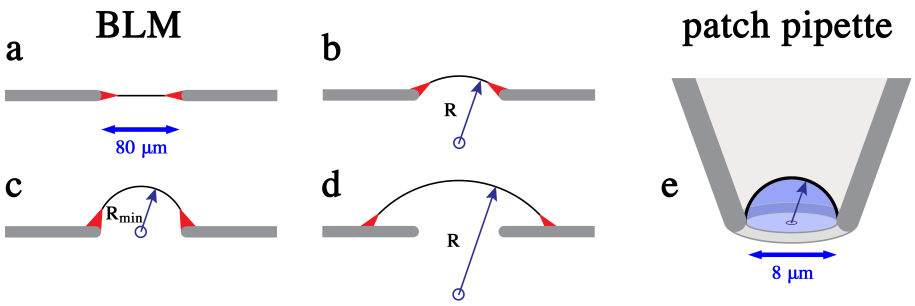

Figure 5. Left: Schematic drawing of a membrane in a BLM measurement. (a) Flat membrane without differences in pressure on the two sides of the membrane. The solvent annulus is shown in in red, an the teflon membrane as a thick grey line. The thin line represents the lipid membrane. (b) In the presence of pressure differences the membranes will bend. (c) The minimum radius of curvature, R_{min} is defined by the dimensions of the hole. Here, it is 40 µm. (d) upon increasing membrane tension, the outer edges of the membranes may slide away from the edges of the hole. Right: The patch pipette has a much smaller diameter. (e) The minimum radius of curvature of the membrane is much smaller, and the curvature much bigger. In the example, the radius of curvature is $\sim$ 4 µm.

(figure 5(a)) and cannot generate an offset potential due to flexoelectricity. However, we often notice in experiments that the membrane bulges out of the plain. The maximum curvature can be expected when the membrane has a radius of curvature similar to the radius of the hole in the membrane (figure 5(c)). All other scenarios lead to smaller curvatures. In figure 5(d) the outer edge of the membrane disconnects from the hole circumference and becomes larger. We often observe this in the experiment. However, in this scenario the curvature becomes smaller. For the present BLM membranes with a diameter of about 80 µm, the minimum radius of curvature is $\sim$ 40 µm. Since the offset potential in the experiment shown in figure 3 is $\Psi_0 = 6mV$, we conclude that for the DMPC:DLPC:cholesterol = 77.3:7.7:15 mixture the flexoelectric coefficient given by $f = \Psi_0\varepsilon_0\varepsilon/(c_1 + c_2)$ is about $3 \cdot 10^{-18}$ C assuming a radius of curvature of $\sim$ 40 µm. We have to conclude that the flexoelectric effect expected for BLM membranes is small because curvatures are small. The patch pipette has a much smaller diameter. The offset potential in the experiment shown in figure 4 is $\Psi_0 = 160mV$. If we assume a minimum radius of curvature of $\sim$ 4 µm, we obtain for the DMPC:DLPC = 90:10 mixture a flexoelectric coefficient of $f = 8.5 \cdot 10^{-18}$ C.

The values for the flexoelectric coefficient given above are lower estimates because we assumed a minimum radius of curvature. However, it is interesting to note that these values are reasonably close to the values for the flexoelectric coefficients found by Todorov and collaborators [18]. They found $f = 4.0 \cdot 10^{-18}$ C for bovine brain PS, $f = 2.6 \cdot 10^{-18}$ C for bacterial PE and $f = 1.8 \cdot 10^{-18}$ C for egg PC. The experiments by Todorov et al. were performed on similar membranes but their measurement included a direct measurement of curvature by optical means. Our experiment is an indirect measurement of curvature because we measure a consequence of flexoelectricity rather than the effect itself. However, the closeness of our numbers for f to Todorov's data suggests that flexoelectricity is a very reasonable explanation for the measured effects, which possesses a significant biological relevance. Our studies point at a direct relevance of flexoelectricity to membrane permeability. I-V profiles observed in biological cells that are outward rectified are usually considered to be a unique feature of proteins. We show here that this is not the case.

In order to quantify our experiments in a better manner it would be useful to measure

the membrane curvature in a direct optical experiment such as the interferometric microscopic methods used by Todorov et al. [18] and then correlate it with the electrophysiological data. Relating this curvature to current-voltage relations may open a new door to interpret electrophysiological experiments with physical methods.

Acknowledgments
This work was supported by the Villum Foundation (VKR 022130).

6. References

[1] Petrov A G 1999 *The lyotropic state of matter. Molecular physics and living matter physics.* (Amsterdam: Gordon and Breach Science Publishers)
[2] Johnston D and Wu S M S 1995 *Cellular Neurophysiology* (Boston: MIT Press)
[3] Hille B 1992 *Ionic channels of excitable membranes* (Cambridge: Cambridge University Press)
[4] Heimburg T and Jackson A D 2005 *Proc. Natl. Acad. Sci. USA* **102** 9790–9795
[5] Andersen S S L, Jackson A D and Heimburg T 2009 *Progr. Neurobiol.* **88** 104–113
[6] Griesbauer J, Bössinger S, Wixforth A and Schneider M F 2012 *Phys. Rev. Lett.* **108** 198103
[7] Griesbauer J, Bössinger S, Wixforth A and Schneider M F 2012 *Phys. Rev. E* **86** 061909
[8] Heimburg T 2012 *Biophys. J.* **103** 918–929
[9] Blicher A, Wodzinska K, Fidorra M, Winterhalter M and Heimburg T 2009 *Biophys. J.* **96** 4581–4591
[10] Heimburg T 2010 *Biophys. Chem.* **150** 2–22
[11] Mosgaard L D and Heimburg T 2013 *Acc. Chem. Res.* **46** 2966–2976
[12] Mosgaard L D, Zecchi K and Heimburg T 2015 *Soft Matter* **11** 7899–7910
[13] Mueller P, Rudin D O, Tien H T and Wescott W C 1962 *Nature* **194** 979–980
[14] Gutsmann T, Heimburg T, Keyser U, Mahendran K R and Winterhalter M 2015 *Nature Protocols* **10** 188–198
[15] Hanke W, Methfessel C, Wilmsen U and Boheim G 1984 *Bioelectrochem. Bioenerg.* **12** 329–339
[16] Laub K R, Witschas K, Blicher A, Madsen S B, Lückhoff A and Heimburg T 2012 *Biochim. Biophys. Acta* **1818** 1–12
[17] Blicher A and Heimburg T 2013 *PloS ONE* **8** e65707
[18] Todorov A, Petrov A G and Fendler J 1994 *Langmuir* **10** 2344–2350
[19] Winterhalter M and Helfrich W 1987 *Phys. Rev. A* **36** 5874–5876
[20] Glaser R W, Leikin S L, Chernomordik L V, Pastushenko V F and Sokirko A I 1988 *Biochim. Biophys. Acta* **940** 275–287
[21] Wodzinska K, Blicher A and Heimburg T 2009 *Soft Matter* **5** 3319–3330